



# Atmospheric buoyancy is likely to influence the amount and intensity of precipitation on the Qinghai-Tibetan Plateau

Progress in Physical Geography  
2025, Vol. 0(0) 1–17  
© The Author(s) 2025  
Article reuse guidelines:  
[sagepub.com/journals-permissions](https://sagepub.com/journals-permissions)  
DOI: 10.1177/03091333251360389  
[journals.sagepub.com/home/ppg](https://journals.sagepub.com/home/ppg)



**Gangfeng Zhang** , **Heyi Yang**, **Xiaokang Hu**, **Jinpeng Hu**, **Jing Yang** and **Daoyi Gong**

State Key Laboratory of Earth Surface Processes and Disaster Risk Reduction, Faculty of Geographical Science, Beijing Normal University, Beijing, China

Academy of Disaster Reduction and Emergency Management, Ministry of Emergency Management & Ministry of Education, Beijing Normal University, Beijing, China

**Lu Jiang**

Academy of Disaster Reduction and Emergency Management, Ministry of Emergency Management & Ministry of Education, Beijing Normal University, Beijing, China

Department of Geography, Liberal Arts College, Beijing Normal University, Zhuhai, China

**Peijun Shi**

State Key Laboratory of Earth Surface Processes and Disaster Risk Reduction, Faculty of Geographical Science, Beijing Normal University, Beijing, China

Academy of Disaster Reduction and Emergency Management, Ministry of Emergency Management & Ministry of Education, Beijing Normal University, Beijing, China

Department of Geography, Liberal Arts College, Beijing Normal University, Zhuhai, China

## Abstract

Precipitation over the Qinghai-Tibetan Plateau is complex and primarily affected by the interaction between atmospheric circulation and the complicated topography due to the high altitude. The impacts of the increased altitudes on precipitation over the Qinghai-Tibetan Plateau remain largely unknown. This study designs numerical simulation experiments in the Weather Research and Forecasting (WRF) model, with actual altitudes reduced by 1000 m, 2000 m, and 3000 m, to simulate convective precipitation on the Qinghai-Tibetan Plateau. Furthermore, the effects of high altitude on convective precipitation were revealed by

## Corresponding authors:

Peijun Shi, State Key Laboratory of Earth Surface Processes and Disaster Risk Reduction, Beijing Normal University, No. 19, Xijiekouwai St, Beijing 100875, China.

Email: [spl@bnu.edu.cn](mailto:spl@bnu.edu.cn)

Lu Jiang, Department of Geography, Liberal Arts College, Beijing Normal University, No.18, Jinfeng Road, Tangjiawan, Zhuhai 519087, China.

Email: [jianglu@bnu.edu.cn](mailto:jianglu@bnu.edu.cn)

analyzing the buoyancy effect combined with the dynamic and thermal effects on precipitation. The results show that altitude has played a crucial role in modulating both convective precipitation intensity and precipitation amount on the Qinghai-Tibetan Plateau. At high altitudes, the water vapour on the Qinghai-Tibetan Plateau was regulated by the high plateau-induced dynamic blocking effect. The high plateau also affects atmospheric lifting conditions through thermal effects, and the atmospheric pressure at the level of free convection was lower due to the decreased atmospheric density and lower atmospheric pressure, forming less energy and weaker buoyancy effects, resulting in a low intensity of convective precipitation and insufficient precipitation amount on the plateau. In the future, it is necessary to add factors such as atmospheric aerosols and atmospheric chemical processes to improve the simulation accuracy and analyze the process of cloud-forming rain caused by convective precipitation on the high-altitude Qinghai-Tibetan Plateau.

## Keywords

Qinghai-Tibetan Plateau, convective precipitation, buoyancy, altitude, numerical simulation

## Introduction

The Qinghai-Tibetan Plateau is an important geomorphic region with an average altitude exceeding 4000 m, known as the ‘third pole of Earth’. The uplift of the Qinghai-Tibetan Plateau is the result of continental collision. Since the end of the Pliocene, the Qinghai-Tibetan Plateau has reached an altitude of 3500–4000 m (Li et al., 1979; Zhong and Ding, 1996). The rise of the Qinghai-Tibetan Plateau significantly changed the surrounding climate system, forming the most powerful Asian monsoon system on Earth (Li and Fang, 1998). The impact of the Qinghai-Tibetan Plateau on climate is mainly manifested in dynamic blocking and thermal effects (Ding, 1991). The primary dynamic effect of the Qinghai-Tibetan Plateau is the mechanical obstruction and friction of atmospheric airflow caused by the high altitude of the plateau terrain, which results in changes in atmospheric dynamic processes. The thermal effect of the Qinghai-Tibetan Plateau is the higher or lower air temperatures on the plateau than in the surroundings during different seasons. In the 1950s, studies focused on the branching and merging effects of Qinghai-Tibetan Plateau dynamics on westerly winds (Bolin, 1950; Gu, 1951; Ye and Gu, 1955). Further studies have found that the dynamic blocking effect of the Qinghai-Tibetan Plateau plays a key role in altering atmospheric circulation, blocking water vapour transport, and causing

drought over the plateau (Ye et al., 1979; Yang et al., 1979; Manabe and Terpstra, 1974; Manabe and Broccoli, 1990).

The Qinghai-Tibetan Plateau can have a significant impact on Asian and global climates through thermal effects (Pan and Li, 1996; Liang et al., 2005). Previous studies have also found significant thermal effects on the Qinghai-Tibetan Plateau over the last few decades. Ye et al., 1957 showed that the Qinghai-Tibetan Plateau was a heat source in summer, with a basic upwards motion, and a cold source in winter, with a downwards motion, based on upper-air and ground data. Later, Ye et al. concluded through a turntable experiment that the East Asian atmospheric circulation and the southwest monsoon were closely related to the thermal effects of the plateau (Ye and Zhang, 1974). Moreover, numerous studies have demonstrated that the thermal effect of the Qinghai-Tibetan Plateau has significantly enhanced the interaction between the lower troposphere and upper troposphere circulation, as well as the interaction between subtropical and tropical monsoon circulation, as a result, the East Asian summer monsoon has intensified, while the South Asian summer monsoon has weakened, and the dry and hot desert climate in Central Asia has experienced further intensification (Duan and Wu, 2005; Wu et al., 2012a; 2012b).

The Qinghai-Tibetan Plateau not only affects the surrounding climate system but also forms a unique plateau climate system. Due to the high altitude, the

air mass above the Qinghai-Tibetan Plateau is only 60% of the sea level (Smith and Shi, 1992), and the precipitation patterns are significantly different from those of low-altitude areas (Li et al., 2012; Luo et al., 2011; Romatschke et al., 2010; Tang et al., 2018a; Yue et al., 2018). The precipitation on the Qinghai-Tibetan Plateau is mainly characterized by convective precipitation, which is much more frequent than that in plain areas at the same latitude due to active convective activities, but its intensity is weak (Ueno et al., 2002; Liu et al., 2002; Xu and Chen, 2006). The daily precipitation on the plateau in summer is often below 10 mm. The weather processes have very few days of daily precipitation exceeding 20 mm (Chang and Guo, 2016; Yan et al., 2016). Studies have shown a correlation between altitude and the frequency and mean intensity of precipitation through statistical data (Zhang, 2019, 2021; Dong and Ni, 2022). Precipitation frequency and mean precipitation intensity likely depend on altitude. Research suggests that the impact of the Qinghai-Tibetan Plateau on precipitation is driven by dynamic and thermal forcing and aerosols changes (Manabe and Terpstra, 1974; Manabe and Broccoli, 1990; Ye et al., 1957; Duan and Wu, 2005; Wu et al., 2012a, 2012b; Lau and Kim, 2006; Xu et al., 2009). Previous studies have rarely focused on the impact of atmospheric buoyancy on plateau precipitation. This article aimed to gain a deeper understanding of the relationship between precipitation and altitude effects on the Qinghai-Tibetan Plateau and to analyze and explore the relationship between altitude and precipitation from the perspective of high altitude and sparse atmosphere.

## Data and methods

### *Meteorological station data*

In this study, the multiyear precipitation data of meteorological stations on the Qinghai-Tibetan Plateau were selected based on the Daily Values of Basic Meteorological Elements from National Weather Stations in China (V3.0) and Hourly Precipitation Data from National Weather Stations in China (V2.0). The data time in the Daily Values of Basic Meteorological Elements from National

Weather Stations in China (V3.0) was 1951–2020, and the data time range in the Hourly Precipitation Data from National Weather Stations in China (V2.0) was 1951–2015. However, there was a large amount of missing data throughout the year at stations on the Qinghai-Tibetan Plateau. To ensure data comparability among stations, the daily data from 1991 to 2020 were selected. For the hourly dataset, the period from June to September of 2007 to 2015 was selected, and the sites with missing data throughout the year that still existed in this time period were removed.

According to the classification of precipitation by the China Meteorological Administration, light rain is defined as daily precipitation less than 10 mm, but the precipitation intensity on the Qinghai-Tibetan Plateau is often small, and precipitation over 10 mm is rare. Most studies use the number of days with daily precipitation greater than 10 mm, the number of days with daily precipitation greater than 20 mm, and the maximum daily precipitation to indicate extreme precipitation on the Qinghai-Tibetan Plateau (You et al., 2008; Wang et al., 2013; Sigdel and Ma, 2017). Based on existing research, this study selected the annual average precipitation, multiyear maximum daily precipitation, multiyear extreme daily precipitation frequency, multiyear maximum hourly precipitation intensity and multiyear extreme hourly precipitation frequency as precipitation indicators to analyze the relationship between precipitation and altitude.

### *WRF mode setting*

In this study, the WRF 4.1 was implemented in conducting the sensitivity experiment. Here we used FNL (Final Operational Global Analysis) data as the meteorological data input and MODIS (Moderate-resolution Imaging Spectroradiometer) 2020 land use data and SRTM (Shuttle Radar Topography Mission) altitude data as static geographic data. The FNL data have a temporal resolution of 6-h and a spatial resolution of  $1^\circ \times 1^\circ$ , and were obtained from the National Centers for Environmental Prediction/National Center for Atmospheric Research (NCEP/

NCAR, <https://rda.ucar.edu/datasets/d083002/#!>). The MODIS data have a spatial resolution of 500 m and were sourced from National Aeronautics and Space Administration (NASA, <https://modis.gsfc.nasa.gov/data/>). The SRTM data have a spatial resolution of 90 m and were obtained from the United States Geological

Survey (USGS, <https://lpdaac.usgs.gov/products/srtmgl3v003/>). The grid design and parameter scheme are shown in Table 1. The simulation area was divided into two layers (Figure 1). The outermost region (d01) covered the Qinghai-Tibetan Plateau and its periphery of approximately 5°, with 146 grids in the east–west direction and 93 grids in the north–south direction, with a grid spacing of 27 km. The second region (d02) covered the entire Qinghai-Tibetan Plateau, with 301 grids in the east–west direction and 190 grids in the north–south direction, with a grid spacing of 9 km. The simulation area is shown in Figure 1. One-way nesting was used between the two layers. To minimize the impact of model errors, a large-scale and high-intensity convective precipitation event that occurred on June 16th on the Tibetan Plateau was specifically selected for analysis. Convective precipitation on June 16, 2020, was selected as a simulation case. On that day, strong convective precipitation occurred on the Qinghai-Tibetan Plateau under the influence of plateau shear at 500 hPa in the middle and high

**Table 1.** Parameterization scheme used for the tests.

WRF 4.1	d01	d02
Number of grids	146 × 95	313 × 199
Grid spacing	27 km	9 km
Time step	120s	40s
Vertical layers	45	
Microphysics	Goddard 4-ice	
Longwave radiation	RRTM	
Shortwave radiation	Dudhia	
Land surface	Noah-MP	
Surface layer	Eta Similarity scheme	
Planetary boundary layer	MYJ	
Cumulus parameterization	Kian-Fritsch(new eat)	

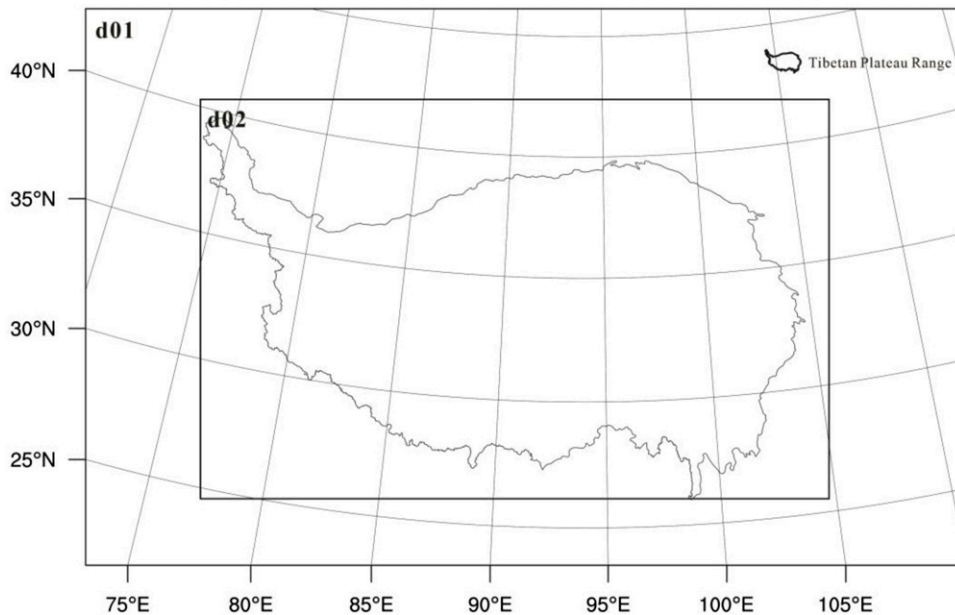


**Figure 1.** Testing range of WRF model. For interpretation of the references to colours in this figure legend, refer to the online version of this article.

latitudes of the Eurasian continent (Deji et al., 2021). The simulation time was from 00:00 June 15 to 00:00 June 17, 2020 (UTC), where the first day was used as the model spin-up time.

In this study, four groups of tests were conducted (Table 2), in which Test 1 was the control group using the altitude data of the actual situation in both nested areas, and Test 2, Test 3 and Test 4 were the experimental groups. In these three groups, the first nested area keeps the actual altitude data, and the second nested area subtracts 1000 m, 2000 m and 3000 m from the actual SRTM data as the altitude data, respectively. As the altitude decreases, some low-altitude regions may yield negative values. To

maintain model stability, we set these negative altitudes to zero.

## Results

### Statistical analysis of the relationship between altitude and precipitation

Recent studies (Chen et al., 2024; Dai et al., 2024; Wang et al., 2024) have evidenced that precipitation exerts increasingly pronounced impacts on agricultural crops and ecosystems under extreme climatic conditions, while the mechanistic uncertainties associated with precipitation-related processes demand further in-depth investigation. Altitude has a crucial effect on precipitation but varies in different regions and scales. The multiyear precipitation amount, precipitation intensity and extreme precipitation frequency of meteorological stations on the Qinghai-Tibetan Plateau significantly declined with increasing altitude (Figure 2). This indicates that precipitation in the Qinghai-Tibetan Plateau is affected by the changed altitude. However, there is no direct causal relationship between altitude and precipitation. The altitude effect influences precipitation by altering the moisture content and thermal conditions in the

**Table 2.** Four sets of nested altitude data for the second layer of experiments.

Test	Altitude data
Test1	Shuttle Radar Topography Mission(SRTM)
Test2	SRTM-1000 m
Test3	SRTM-2000 m
Test4	SRTM-3000 m

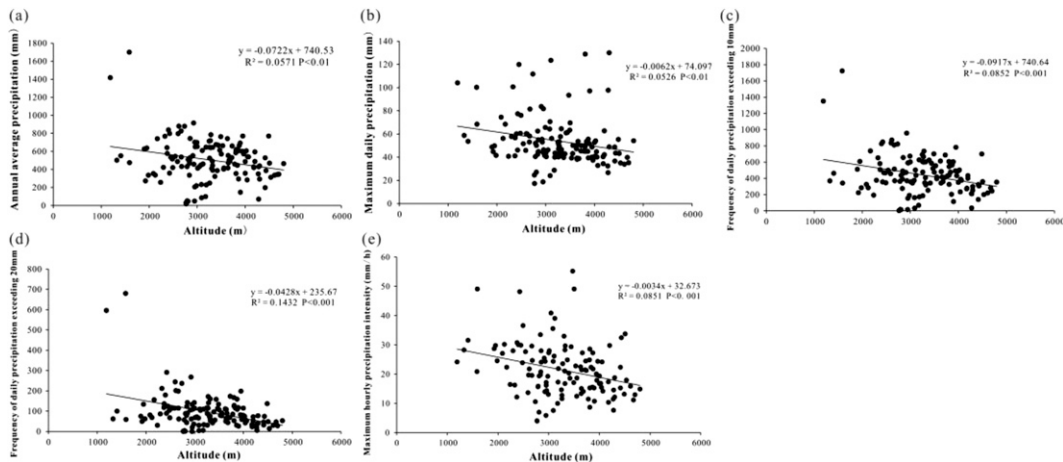


**Figure 2.** Relationship between precipitation and altitude over the Qinghai-Tibetan Plateau. (a) The relationship between annual precipitation and altitude. (b) The relationship between maximum daily precipitation and altitude. (c) The relationship between the frequency of daily precipitation exceeding 10 mm and altitude. (d) The relationship between the frequency of daily precipitation exceeding 20 mm and altitude. (e) The relationship between maximum hourly precipitation intensity and altitude.

atmosphere. Early studies also indicated that the relationship between altitude and precipitation varies across different regions (Zhang, 2019, 2021; Dong and Ni, 2022). When analyzing the annual precipitation statistical data of the Qinghai-Tibetan Plateau, we reduced the original altitude by 1000 m, 2000 m, and 3000 m and examined the relationship between altitude and precipitation indicators. We found that the relation between the altitude and the average annual precipitation and the maximum daily precipitation over the years become weak gradually (Figure S1).

### *Correlation between altitude changes and single precipitation revealed by numerical simulation*

Inspired by the aforementioned statistical results, this study chose a single convective precipitation event to further explore the impact of altitude on precipitation by conducting sensitivity experiments in the WRF model.

The changes in precipitation and precipitation intensity with altitude were analyzed by calculating the maximum 24-h cumulative precipitation, the precipitation area where the 24-h cumulative precipitation exceeded 25 mm and 50 mm, the maximum hourly precipitation intensity, the precipitation area where the maximum hourly precipitation intensity exceeded 16 mm/h, the maximum average hourly precipitation intensity and the precipitation area where the average hourly precipitation intensity exceeded 5 mm/h. Statistics of precipitation indicators under different tests are shown in Table 3. The results (Figure 3 and Table 3) showed that the maximum 24-h cumulative precipitation in Test 1 decreased by 139.27 mm, 225.05 mm and 234.7 mm compared with Test 2, Test 3 and Test 4,

respectively; the precipitation area with 24-h cumulative precipitation over 25 mm in Test 1 decreased by 40,581 km<sup>2</sup>, 90,072 km<sup>2</sup> and 87,075 km<sup>2</sup> compared with Test 2, Test 3 and Test 4, respectively; and the 24-h cumulative precipitation area exceeding 50 mm in Test 1 decreased by 14,337 km<sup>2</sup>, 34,911 km<sup>2</sup> and 37,989 km<sup>2</sup> compared with Test 2, Test 3 and Test 4, respectively. With increasing altitude (Test 4 to Test 1), the maximum 24-h cumulative precipitation decreased by 3.2%, 31.5% and 77.4%, respectively. Furthermore, another case on July 14, 2019 also shows a similar pattern of precipitation in various tests (Figure S2), indicating the robustness of the effect of elevation changes on precipitation.

The indicators associated with maximum hourly precipitation intensity in 24 hours are shown in Table 4. The results (Figure 4 and Table 4) showed that with increasing altitude, the maximum hourly precipitation intensity of Test 1 decreased by 22.36 mm/h, 43.04 mm/h and 56.32 mm/h relative to the precipitation of Test 2, Test 3 and Test 4, respectively; the precipitation area with maximum hourly precipitation intensity exceeding 16 mm/h decreased by 17,577 km<sup>2</sup>, 26,325 km<sup>2</sup> and 42,120 km<sup>2</sup>, compared with Test 2, Test 3 and Test 4, respectively. With increasing altitude (Test 4 to Test 1), the maximum hourly precipitation intensity decreased by 14.1%, 36.0% and 59.6%, respectively.

The relevant indicators of average hourly precipitation intensity in 24 hours are displayed in Table 5. The average hourly precipitation intensity result (Figure 5 and Table 5) showed that with increasing altitude, the maximum average hourly precipitation intensity in Test 1 decreased by 4.74 mm/h, 11.21 mm/h, and 19.24 mm/h compared

**Table 3.** Convective precipitation index of the Qinghai-Tibetan Plateau under different tests.

	Maximum precipitation (mm)	24-h accumulated precipitation over 25 mm area (km <sup>2</sup> )	24-h accumulated precipitation over 50 mm area (km <sup>2</sup> )
Test 1	68.48	59,211	1539
Test 2	207.75	99,792	15,876
Test 3	293.53	149,283	36,450
Test 4	303.18	146,286	39,528



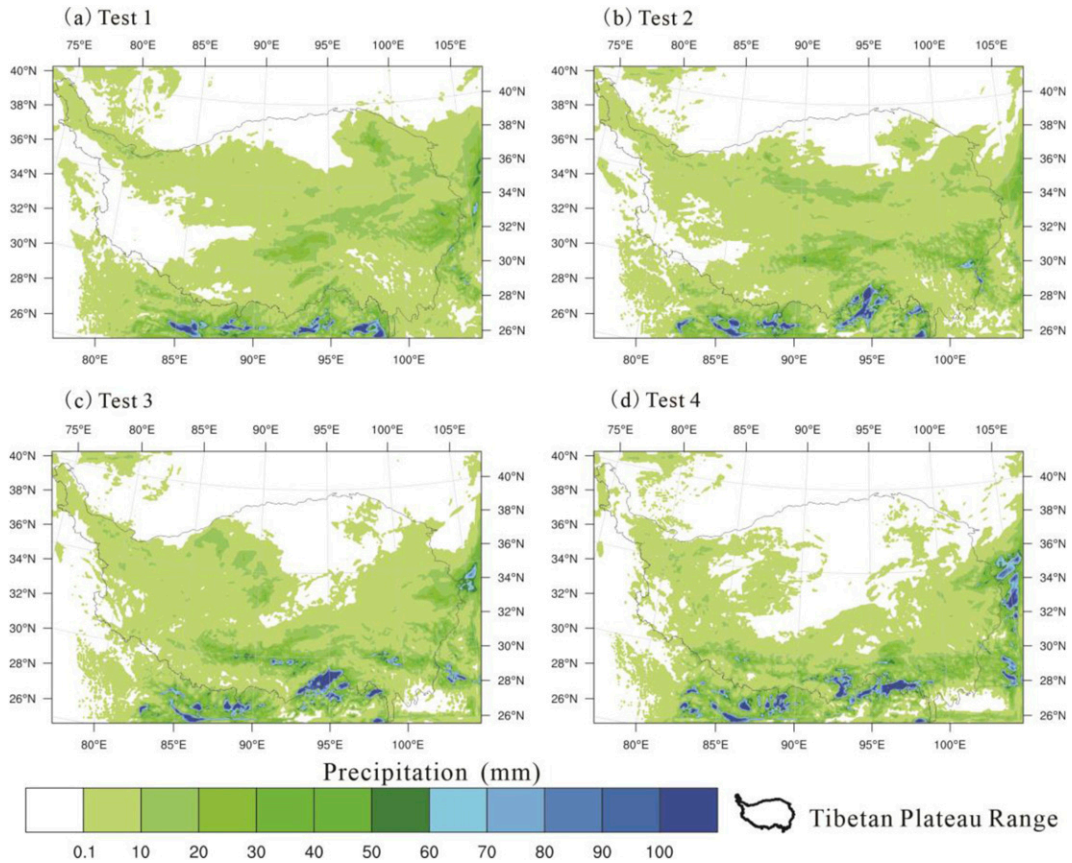


**Figure 3.** 24-h cumulative precipitation in different tests on June 16, 2020. For interpretation of the references to colours in this figure legend, refer to the online version of this article.

**Table 4.** Maximum hourly precipitation intensity index of convective precipitation in the Qinghai-Tibetan Plateau under different tests.

	Maximum hourly precipitation intensity (mm/h)	Area with maximum hourly precipitation intensity exceeding 16 mm/h (km <sup>2</sup> )
Test 1	38.11	2349
Test 2	60.47	15,228
Test 3	81.15	28,674
Test 4	94.43	44,469

with Test 2, Test 3, and Test 4, respectively; the precipitation area with an average hourly precipitation intensity exceeding 5 mm/h in Test 1 decreased by 7290 km<sup>2</sup>, 17,739 km<sup>2</sup>, and 36,855 km<sup>2</sup> compared with Test 2, Test 3, and Test 4, respectively. With

increasing altitude (Test 4 to Test 1), the average hourly precipitation intensity decreased by 32.9, 59.4% and 79.5%, respectively.

The comparison implied that the increase in altitude of the Qinghai-Tibetan Plateau led to a

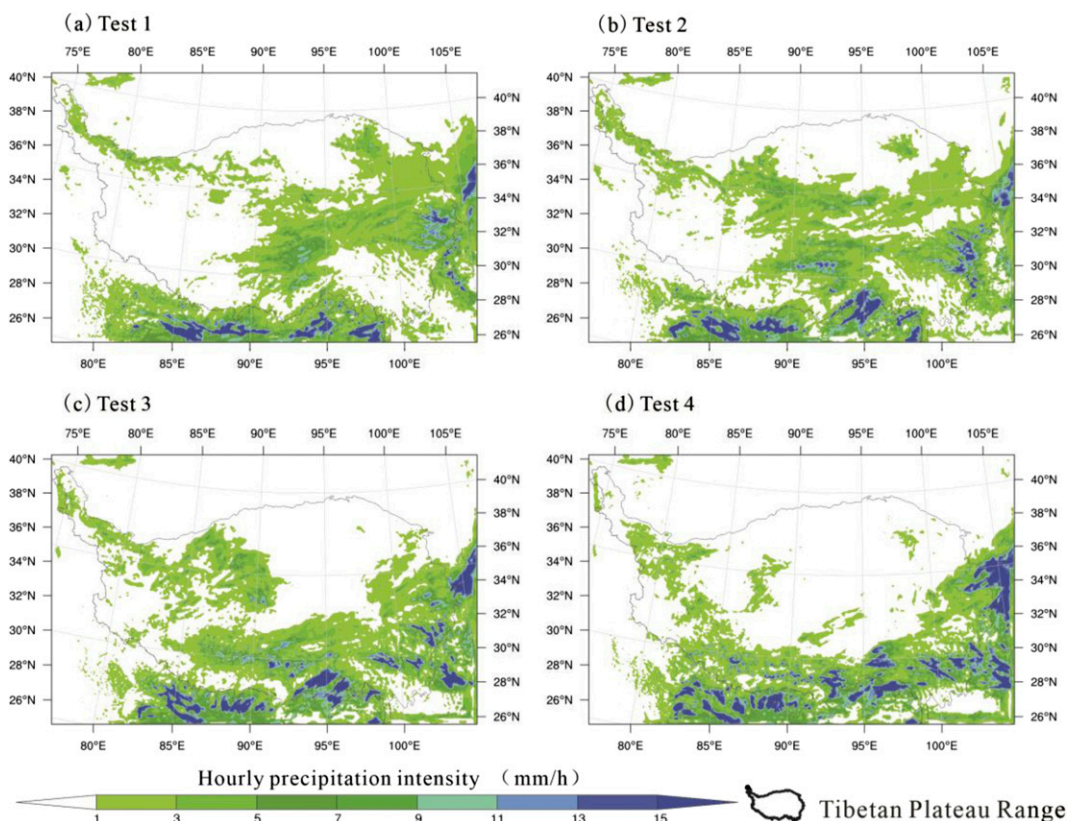


**Figure 4.** Maximum hourly precipitation intensity for different tests on June 16, 2020. For interpretation of the references to colours in this figure legend, refer to the online version of this article.

**Table 5.** Average hourly precipitation intensity index of convective precipitation in the Qinghai-Tibetan Plateau under different tests.

	Maximum average hourly precipitation intensity (mm/h)	Precipitation area with average hourly precipitation intensity exceeding 5 mm/h (km <sup>2</sup> )
Test 1	5.16	324
Test 2	9.90	7614
Test 3	16.37	18,063
Test 4	24.40	37,179

decrease in both the amount and the intensity of convective precipitation, and the high altitude was likely the primary driver of this convective precipitation characteristic on the Qinghai-Tibetan Plateau.

This dependence of precipitation on altitude over the Qinghai-Tibetan Plateau has also been shown in other studies (Tang et al., 2018b; Dong and Ni, 2022; Zhang et al., 2023).



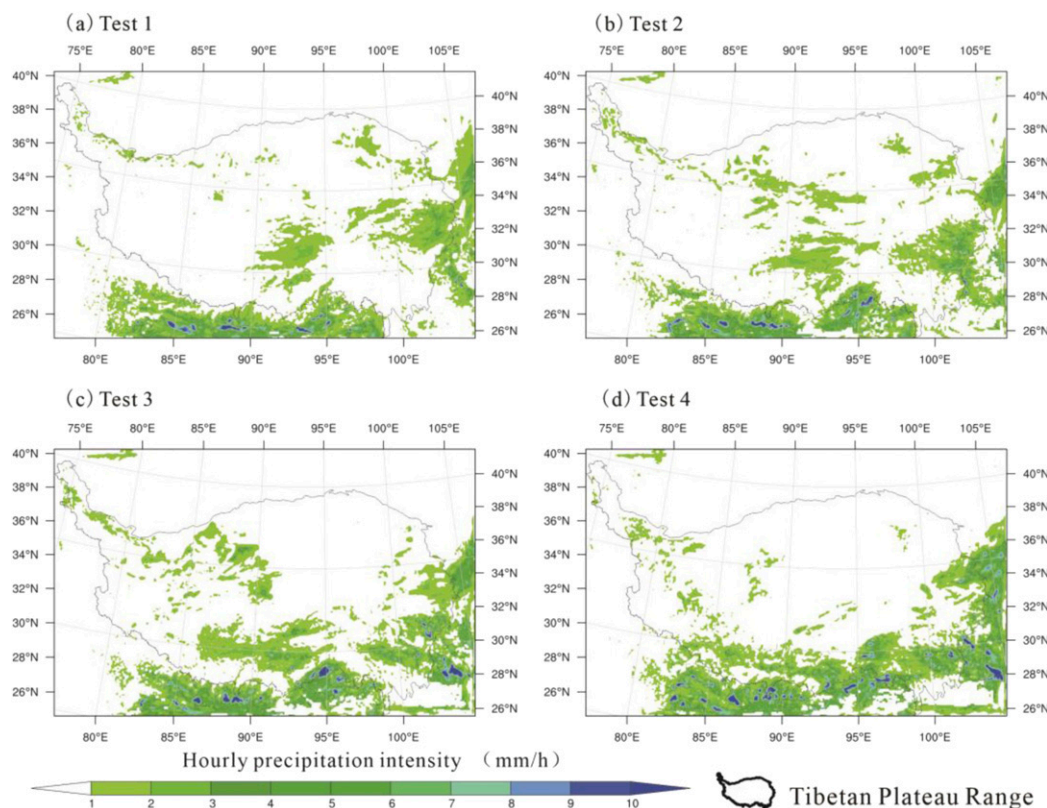


**Figure 5.** Mean hourly precipitation intensity for different tests on June 16, 2020. For interpretation of the references to colours in this figure legend, refer to the online version of this article.

### Verification of model simulations

To verify the simulation effect of the model for these precipitation events, the results of Test 1 (actual altitude) were compared with the observation data of meteorological stations and reanalysis data. The results are shown in Figure S3 by comparing the cumulative precipitation observed at the meteorological station on June 16, 2020, with the simulation results. The correlation coefficient between the simulation and the observation was 0.64 ( $p < .01$ ). The root mean square error was 6.33, and the average absolute error was 4.53.

The hourly precipitation distribution from the precipitation fusion product of the China Meteorological Administration Land Surface Data Assimilation System (CLDAS) was compared with the hourly precipitation distribution from Test 1 (actual

altitude) to verify the reliability of the simulations, which are shown in Figure S4. First, the precipitation from CLDAS formed and gradually intensified in the northeastern part of the plateau and then formed in the central part of the plateau at approximately 12:00 a.m. The precipitation gradually weakened in the eastern part at 18:00 p.m. and mostly weakened and stopped on the Qinghai-Tibetan Plateau by 22:00 p.m. In the WRF simulation results (Figure S4), WRF basically simulated the process of this precipitation. Compared with the observations, the precipitation was more extensive and intense, especially in the central part of the plateau. However, the occurrence and end time of the precipitation basically coincided, so the model could reproduce the process of this precipitation.

Furthermore, the hourly precipitation area in the WRF simulation was statistically compared with the

hourly results of CLDAS. The results showed that (Figure S5) the WRF and CLDAS in the main areas of precipitation (eastern, central and northeast of the plateau) showed a significant correlation ( $r > 0.8$ ,  $p < .05$ ). There was a negative correlation between the WRF and CLDAS in some regions because there was an error in precipitation time between the WRF and CLDAS. Overall, most regions showed a significant positive correlation.

### Physical processes behind altitude induced precipitation changes

The water transport on the windward slope of the plateau plays an important role in the precipitation of the plateau (Li et al., 2024). The dynamic processes of the Qinghai-Tibetan Plateau affect the water vapour transfer of the plateau by blocking atmospheric circulation. By calculating the difference in precipitable water in the four groups of tests, it was found (Figure 6) that with the decline in altitude, the precipitable water in the whole Qinghai-Tibetan Plateau increased, and the increase in precipitable water in the southeastern part was much larger than that in the northwestern part. By calculating the water vapour flux at the lowest level of the model, it was observed (Figure 7) that the transport of water vapour in the near-surface region of the Qinghai-Tibetan Plateau increased gradually with decreasing altitude. The decrease in altitude not only increases the atmospheric thickness below 5 km, but also weakens the plateau's dynamic barrier, allowing more water

vapour from the sea to enter the interior of the plateau. The increase in precipitable water provided more water vapour for convective precipitation, which was also an important factor for the increase in convective precipitation with decreasing altitude.

By calculating the variations in sensible heat flux and latent heat flux between different tests, it was found that with decreasing altitude, the sensible heat flux in most regions of the Qinghai-Tibetan Plateau gradually decreased (Figure S6), while the latent heat flux increased (Figure S7). The enhancement of sensible heat flux over the Qinghai-Tibetan Plateau can strengthen the upwards movement of air masses (Zhang and Klein, 2010; Tang et al., 2023). By calculating the distribution of the maximum vertical wind speed on June 16th, 2020 in four groups of tests, the changes in convective precipitation uplift conditions at different altitudes were explored. The presence of more extensive updrafts creates favourable thermodynamic conditions for convective initiation, thereby driving the development of spatially expansive convective systems. The results (Figure 8) showed that the Qinghai-Tibetan Plateau produced a wider range of updrafts through the thermal effect of high altitude, which played a key role in convective precipitation.

The dynamic and thermal effects on the Qinghai-Tibetan Plateau are a fundamental research direction in the study of weather and climate on the plateau. In addition to these two effects, the high altitude of the Qinghai-Tibetan Plateau will change the physical properties of the atmosphere. For example, an increase in altitude will reduce the atmospheric density,

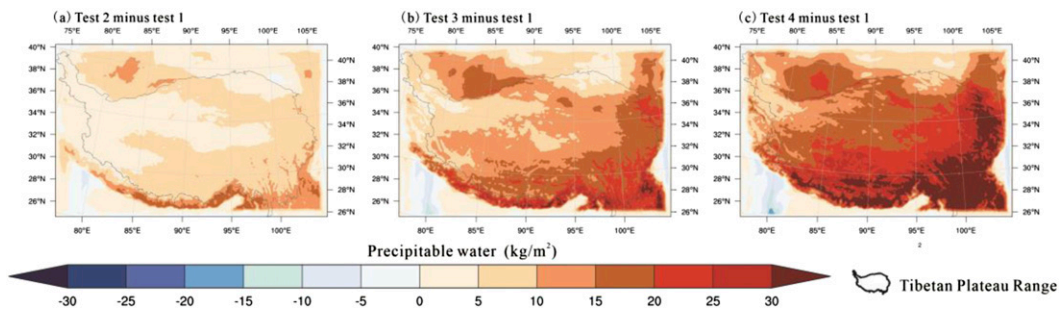


**Figure 6.** Difference in hourly average precipitable water in four groups of tests on June 16, 2020. For interpretation of the references to colours in this figure legend, refer to the online version of this article.

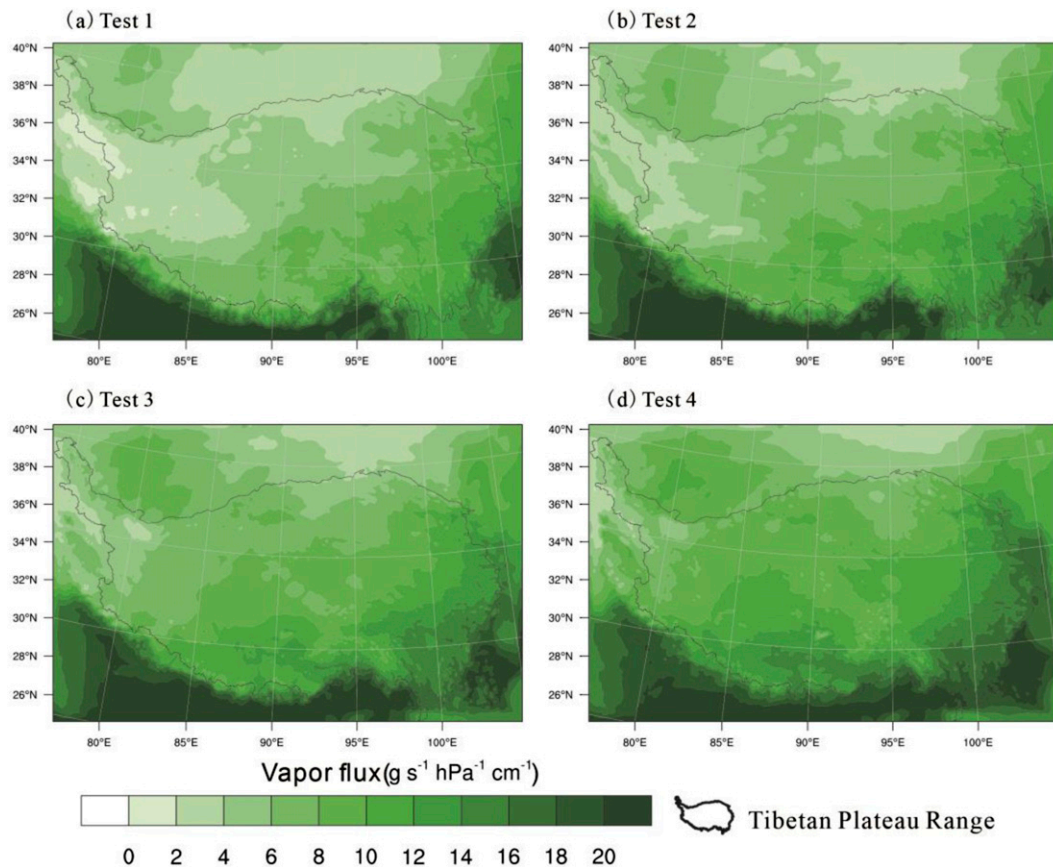


**Figure 7.** Average bottom vapour flux in four groups of tests on June 16th, 2020. For interpretation of the references to colours in this figure legend, refer to the online version of this article.

make the air thinner, and reduce the atmospheric pressure, which will lead to a change in the buoyancy effect of the atmosphere. Therefore, this article analyzed the results of different tests through level of free convection and convective available potential energy and explored the influence of buoyancy on precipitation and precipitation intensity.

Figure S8 shows the average level of free convection of all grid points in four sets of tests on June 16<sup>th</sup>, where negative buoyancy acted below the level of free convection and positive buoyancy acted above the level of free convection. According to the results (Figure S8), with the altitude increased, the level of free convection also increased. Level of free convection was detected in the southern part of the

plateau where the precipitation area was located. Therefore, convective precipitation on the Qinghai-Tibetan Plateau at high altitudes had a higher level of free convection from the ground, and air masses needed to rise to a higher height to enter a state of positive buoyancy.

The entire atmospheric conditions between the level of free convection and the equilibrium level determine the magnitude of the energy. By converting the level of free convection into the corresponding atmospheric pressure, we can explore the changes in the atmosphere above the level of free convection. As shown in Figure S9, with increasing altitude, the atmospheric pressure at the level of free convection gradually decreased, indicating that the atmospheric pressure above the level of free

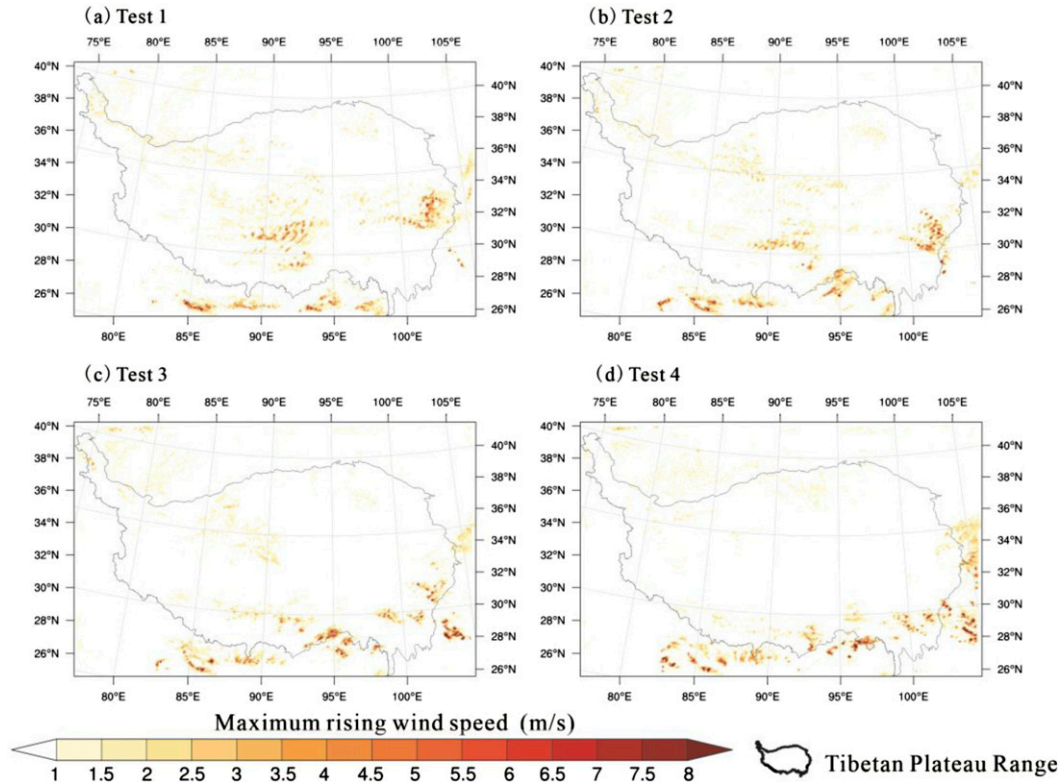


**Figure 8.** The hourly average maximum vertical wind speed in the four groups of tests on June 16th, 2020. For interpretation of the references to colours in this figure legend, refer to the online version of this article.

convection was lower, and the buoyancy was also smaller.

The convective available potential energy reflects the magnitude of the action done by positive buoyancy. The calculation of convective available potential energy specifically shows how the action of positive buoyancy changes with increasing altitude and further delves the buoyancy change into the energy change. Figure 9 shows that the convective available potential energy decreased and became more dispersed as the altitude increased. Buoyancy analysis indicates that increased altitude raises the height of free convection, reducing atmospheric pressure above this level. This decrease in buoyancy lowers convective available potential energy, weakening energy conditions in the atmosphere and hindering the formation of unstable stratification and strong convection. By modulating energy, buoyancy

directly influences convective precipitation intensity, making it a key factor in high-altitude precipitation on the Qinghai-Tibetan Plateau.

## Discussion

In this study, the dynamic, thermal and buoyant effects of the Qinghai-Tibetan Plateau represented the physical mechanism of the altitude effect on precipitation. These three processes affected the convective precipitation of the Qinghai-Tibetan Plateau by changing the water vapour conditions, uplift conditions and unstable stratification of convective precipitation. This study only demonstrated the influence of buoyancy on plateau precipitation through comparative numerical simulations, but did not delve into the atmospheric physical processes of buoyancy affecting precipitation. While various



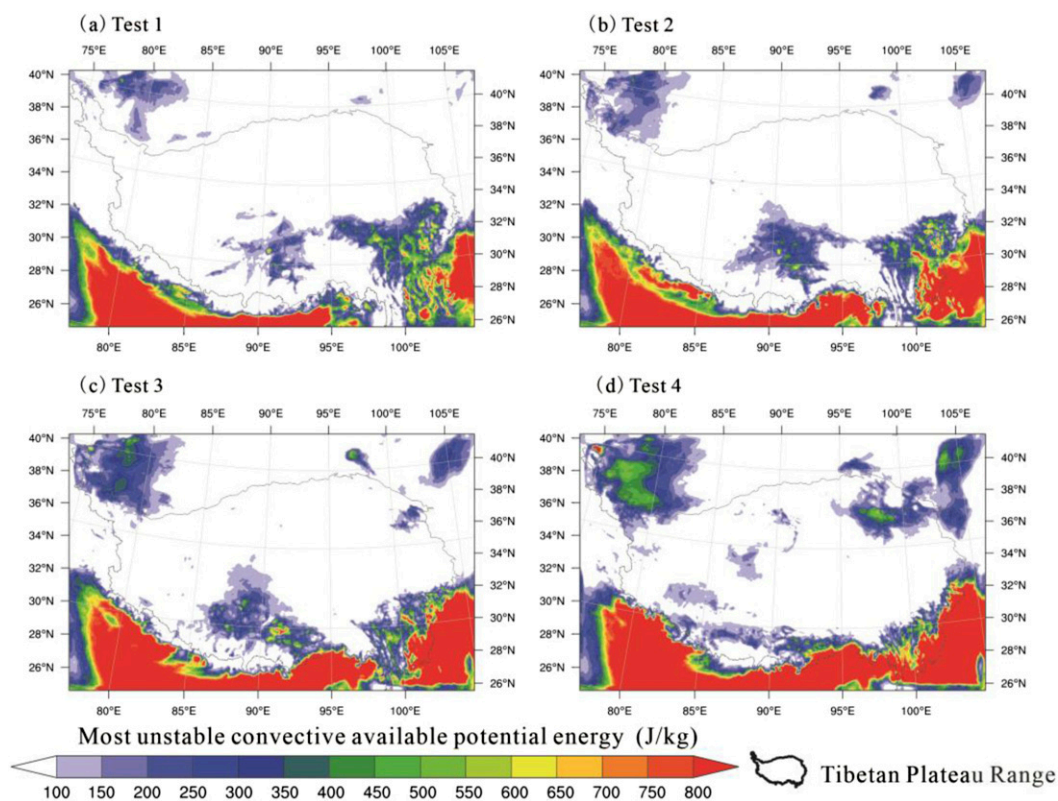


**Figure 9.** Hourly average most unstable convective available potential energy of four groups of tests on June 16th, 2020. For interpretation of the references to colours in this figure legend, refer to the online version of this article.

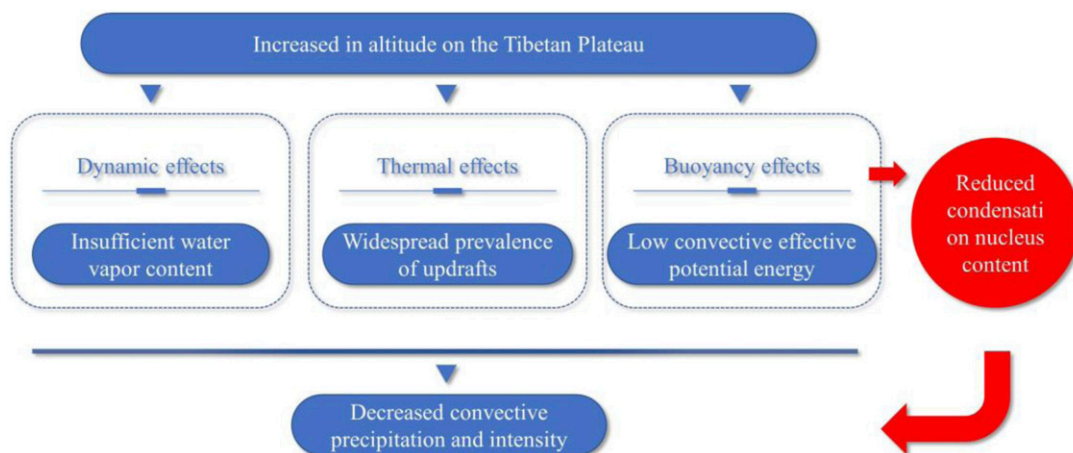


**Figure 10.** The mechanism of altitude affecting precipitation. For interpretation of the references to colours in this figure legend, refer to the online version of this article.



factors influencing precipitation patterns are being examined, the specific significance of each factor has not been quantified and warrants further investigation. Note that a resolution of 9 km may not accurately capture the dynamics of updrafts and downdrafts, leading to convective processes largely overlooking entrainment processes. Furthermore, many anthropogenical factors can also affect convective precipitation on the Qinghai-Tibetan Plateau but were not considered in our study. The important factor was the influence of atmospheric aerosols and related atmospheric chemical processes on precipitation. Atmospheric aerosols cannot only provide necessary condensation for precipitation but also affect the formation of precipitation by changing atmospheric composition, atmospheric visibility and solar radiation. Extensive research has demonstrated that aerosols significantly influence the climate of the Qinghai-Tibetan Plateau (Lau and Kim, 2006; Xu et al., 2009; Fang et al., 2015). Further research on the role of atmospheric aerosols in convective precipitation over the Qinghai-Tibetan Plateau is strongly needed. Our study retained the original terrain of the Qinghai-Tibetan Plateau in the simulation process and only changed the altitude, while the internal terrain of the Qinghai-Tibetan Plateau is complex. Whether the impact of altitude on convective precipitation will exist within the plateau due to the terrain also needs further study.

Given that the initial fields remain unchanged, any adjustment in altitude results in discrepancies in the altitudes of meteorological elements at the domain boundaries, thereby introducing biases into the simulations. Such altitude differences between the inner and outer domains are an inherent limitation of regional models. However, exploring these issues in the global models could be a potential avenue for future research. Due to the high altitude and complex topography on the Qinghai-Tibetan Plateau, there was a certain uncertainty between the simulation results and the actual situation. The static geographic data (land use, soil, etc.) used in the simulation were quite different from the actual situation, the terrain undulation was large and the resolution was insufficient, the WRF simulation driving data had a certain error, and when WRF simulated lake temperature, it

did not consider altitude, and the parameter scheme of WRF had difficulty reflecting the actual physical process. Note that the current simulation setup prioritizes a large spatial domain with coarser resolution (27 km), which necessitated a compromise in strictly adhering to the 1:3 nesting ratio between domains. This may potentially introduce some bias into the downscaling process. Future high-resolution modelling investigations can systematically address and optimize these scaling considerations to further enhance the accuracy and reliability of the simulation results.

## Conclusion

This study designed four sets of convective precipitation experiments on the Qinghai-Tibetan Plateau at different altitudes. From the 24-h cumulative precipitation, maximum hourly precipitation intensity, and average hourly precipitation intensity, it can be seen that as the altitude increased, the 24-h cumulative precipitation and hourly precipitation intensity of convective precipitation on the Qinghai-Tibetan Plateau showed downwards trends. High altitude can respond to the insufficient and low intensity of convective precipitation on the Qinghai-Tibetan Plateau. Based on the analysis of the dynamic, thermal, and buoyancy effects on the Qinghai-Tibetan Plateau, this study summarized the potential causes behind the decrease in precipitation and intensity of convective precipitation over the Qinghai-Tibetan Plateau with increasing altitude from the changes in convective precipitation water vapour conditions, uplift conditions, and unstable stratification at different altitudes. The mechanism is shown in Figure 10. First, the dynamic blocking effect of the Qinghai-Tibetan Plateau resulted in insufficient precipitable water and insufficient water vapour on the plateau. Second, the thermal effect of the Qinghai-Tibetan Plateau led to the widespread prevalence of updrafts. Meanwhile, due to its high altitude, low atmospheric pressure, low atmospheric density, insufficient positive buoyancy work, and low convective effective potential energy, the combined effect of thermal and buoyancy makes it difficult for the Qinghai-Tibetan Plateau to develop

stronger convection despite having certain uplift conditions. The combined effects of dynamics, thermal, and buoyancy have led to the convective precipitation characteristics of the Qinghai-Tibetan Plateau. The buoyancy effect caused by the increase in altitude and the thinning of the atmosphere is an important driver of the frequent but insufficient intensity of convective activities in the Qinghai-Tibetan Plateau. At the same time, we think the weak buoyancy caused by high altitude may also affect the concentration of condensation nuclei in the atmosphere, leading to insufficient condensation nuclei, making it difficult to form stronger and more precipitation. This is also the focus of our next research direction. The importance of buoyancy in meteorological research on the Qinghai-Tibetan Plateau should be emphasized.

### Acknowledgements

The authors wish to acknowledge the editor and the anonymous reviewers for their detailed and helpful comments to the original manuscript.

### Declaration of conflicting interests

The authors declared no potential conflicts of interest with respect to the research, authorship, and/or publication of this article.

### Funding

The authors disclosed receipt of the following financial support for the research, authorship, and/or publication of this article: This research was supported by the Second Tibetan Plateau Scientific Expedition and Research Program (STEP, 2019QZKK0606), Qinghai Provincial Central Government-Guided Local Science and Technology Development Fund - Science and Technology Innovation Base Construction Project (2025ZY017), and the National Natural Science Foundation of China (42330502, 42101027).

### ORCID iDs

Gangfeng Zhang  <https://orcid.org/0000-0003-4788-0394>

Peijun Shi  <https://orcid.org/0000-0002-2968-7331>

### Supplemental Material

Supplemental material for this article is available online.

### References

- Bolin B (1950) On the influence of the earth's orography on the westerlies. *Tellus* 2: 184–195.
- Chang Y and Guo X (2016) Characteristics of convective cloud and precipitation during summer time at Naqu over Tibetan Plateau (in Chinese). *Chinese Science Bulletin* 61: 1706–1720.
- Chen XX, Wang LC, Cao Q, et al. (2024) Response of global agricultural productivity anomalies to drought stress in irrigated and rainfed agriculture. *Science China Earth Sciences* 69: 3579–3593.
- Dai X, Wang LC, Gong J, et al. (2024) Extreme weather characteristics and influences on urban ecosystem services in Wuhan Urban Agglomeration. *Geography and Sustainability* 6: 100201.
- Deji B, Ciren L, Zhuo M, et al. (2021) Diagnostic analysis of a heavy rainfall in the southeast of Naqu (in Chinese). *Tibet Science and Technology* 03: 19–21+27.
- Ding YH (1991) *Advanced Synoptic Meteorology*. Beijing: China Meteorological Press, 663–664.
- Dong X and Ni X (2022) Spatiotemporal variation of extreme precipitation at different elevations in southwest China (in Chinese). *Journal of Southwest University (Natural Science)* 44: 110–121.
- Duan AM and Wu GX (2005) Role of the Tibetan Plateau thermal forcing in the summer climate patterns over subtropical Asia. *Climate Dynamics* 24: 793–797.
- Fang KY, Makkonen R, Guo ZT, et al. (2015) An increase in the biogenic aerosol concentration as a contributing factor to the recent wetting trend in Tibetan Plateau. *Scientific Reports* 5: 14628.
- Gu ZC (1951) The dynamic impact of the Tibetan Plateau on the East Asian circulation and its importance (in Chinese). *Scientia Sinica* 03: 283–303.
- Lau K-M and Kim K-M (2006) Observational relationships between aerosol and Asian monsoon rainfall, and circulation. *Geophysical Research Letters* 33: 21810-1–21810-5.
- Li JJ and Fang XM (1998) Research on the uplift of the Qinghai Tibet Plateau and environmental changes (in Chinese). *Chinese Science Bulletin* 15: 1569–1574.

- Li JJ, Wen SX, Zhang QS, et al. (1979) An exploration of the age, magnitude and form of the Tibetan Plateau uplift (in Chinese). *Scientia Sinica* 06: 608–616.
- Li D, Bai AJ and Huang SJ (2012) Characteristic analysis of a severe convective weather over Tibetan Plateau based on TRMM data (in Chinese). *Plateau Meteorology* 31: 304–311.
- Li J, Lu C, Chen J, et al. (2024) The influence of complex terrain on cloud and precipitation on the foot and slope of the southeastern Tibetan Plateau. *Climate Dynamics* 62: 3143–3163.
- Liang XY, Liu QM and Wu GX (2005) Effect of Tibetan Plateau on the site of onset and intensity of the Asian summer monsoon (in Chinese). *Acta Meteorologica Sinica* 05: 799–805.
- Liu LP, Feng JM, Chu SZ, et al. (2002) The diurnal variation of precipitation in monsoon season in the Tibetan Plateau. *Advances in Atmospheric Sciences* 19: 365–378.
- Luo Y, Zhang R, Qian W, et al. (2011) Intercomparison of deep convection over the Tibetan Plateau-Asian monsoon region and subtropical North America in boreal summer using CloudSat/CALIPSO data. *Journal of Climate* 24: 2164–2177.
- Manabe S and Broccoli AJ (1990) Mountains and arid climates of middle latitudes. *Science* 247: 192–194.
- Manabe S and Terpstra TB (1974) The effects of mountains on the general circulation of the atmosphere as identified by numerical experiments. *Journal of the Atmospheric Sciences* 31: 3–42.
- Pan BT and Li JJ (1996) Qinghai-Tibetan plateau: a driver and amplifier of the global climatic change (in Chinese). *Journal of Lanzhou University (Natural Sciences)* 01: 108–115.
- Romatschke U, Medina S and Houze RA (2010) Regional, seasonal, and diurnal variations of extreme convection in the South Asian region. *Journal of Climate* 23: 419–439.
- Sigdel M and Ma YM (2017) Variability and trends in daily precipitation extremes on the northern and southern slopes of the central Himalaya. *Theoretical and Applied Climatology* 130: 571–581.
- Smith EA and Shi L (1992) Surface forcing of the infrared cooling profile over the Tibetan plateau. Part I: influence of relative longwave radiative heating at high altitude. *Journal of the Atmospheric Sciences* 49: 805–822.
- Tang J, Guo XL and Chang Y (2018a) Cloud microphysics and regional water budget of a summer precipitation process at Naqu over the Tibetan Plateau (in Chinese). *Chinese Journal of Atmospheric Sciences* 42: 1327–1343.
- Tang GQ, Long D, Hong Y, et al. (2018b) Documentation of multifactorial relationships between precipitation and topography of the Tibetan Plateau using spaceborne precipitation radars. *Remote Sensing of Environment* 208(1): 82–96.
- Tang S, Vlug A, Piao S, et al. (2023) Regional and teleconnected impacts of the Tibetan Plateau surface darkening. *Nature Communications* 14: 32.
- Ueno K, Fujii H, Yamada H, et al. (2002) Weak and frequent monsoon precipitation over the Tibetan plateau. *Journal of the Meteorological Society of Japan. Ser. II* 79: 419–434.
- Wang SJ, Zhang MJ, Wang BL, et al. (2013) Recent changes in daily extremes of temperature and precipitation over the western Tibetan Plateau, 1973–2011. *Quaternary International* 313: 110–117.
- Wang LC, Zhong DH, Chen XX, et al. (2024) Impact of climate change on rice growth and yield in China: analysis based on climate year type. *Geography and Sustainability* 5: 548–560.
- Wu G, Liu Y, Dong B, et al. (2012a) Revisiting Asian monsoon formation and change associated with Tibetan Plateau forcing: I. Formation. *Climate Dynamics* 39: 1169–1181.
- Wu G, Liu Y, He B, et al. (2012b) Thermal controls on the Asian summer monsoon. *Scientific Reports* 2: 404.
- Xu XD and Chen LS (2006) Advances of the study on Tibetan Plateau experiment of atmospheric sciences (in Chinese). *Journal of Applied Meteorological Science* 06: 756–772.
- Xu B, Cao J, Hansen J, et al. (2009) Black soot and the survival of Tibetan glaciers. *Proceedings of the National Academy of Sciences of the United States of America* 106: 22114–22118.
- Yan Y, Liu Y and Lu J (2016) Cloud vertical structure, precipitation, and cloud radiative effects over Tibetan Plateau and its neighboring regions. *Journal of Geophysical Research: Atmospheres* 121: 305–323.
- Yang GJ, Wang XD and Ye DZ (1979) The average vertical circulation over the east-Asia and the pacific area (2) winter (in Chinese). *Chinese Journal of Atmospheric Sciences* 04: 299–305.

- Ye DZ and Gu ZC (1955) The impact of the Tibetan Plateau on the atmospheric circulation in East Asia and the weather in China (in Chinese). *Chinese Science Bulletin* 06: 29–33.
- Ye D and Zhang JQ (1974) Preliminary simulation experiments on the influence of heating on the summer East Asian atmospheric circulation over the Qinghai-Tibet Plateau (in Chinese). *Scientia Sinica* 03: 301–320.
- Ye DZ, Luo SW and Zhu BZ (1957) The wind structure and heat balance in the lower troposphere over Tibetan Plateau and its surrounding (in Chinese). *Acta Meteorologica Sinica* 02: 108–121.
- Ye DZ, Yang GJ and Wang XD (1979) The average vertical circulations over the East-Asia and the Pacific area, (I) in summer (in Chinese). *Chinese Journal of Atmospheric Sciences* 01: 1–11.
- You Q, Kang S, Aguilar E, et al. (2008) Changes in daily climate extremes in the eastern and central Tibetan Plateau during 1961–2005. *Journal of Geophysical Research: Atmospheres* 113: D07101.
- Yue ZG, Yu X, Liu GH, et al. (2018) NPP/VIIRS satellite retrieval of summer convective cloud microphysical properties over the Tibetan Plateau (in Chinese). *Acta Meteorologica Sinica* 76: 968–982.
- Zhang MM (2019) The relationship between precipitation and altitude over east of the Tibetan Plateau. *Chinese Academy of Meteorological Sciences*, (in Chinese).
- Zhang Y and Klein S (2010) Mechanisms affecting the transition from shallow to deep convection over land: inferences from observations of the diurnal cycle collected at the ARM southern great plains site. *Journal of the Atmospheric Sciences* 67: 2943–2959.
- Zhang MM, Li J, Gan YT, et al. (2021) Analysis of the relationship between precipitation and altitude over central and eastern China based on the Geographically Weighted Regression Model (in Chinese). *Torrential Rain and Disasters* 40: 1–11.
- Zhang WQ, Liu L, Lun YR, et al. (2023) Elevation-dependent precipitation variability over the Tibetan Plateau: a synthesis of observations and high-resolution simulations (in Chinese). *Journal of Soil and Water Conservation* 02: 149–158+216.
- Zhong DL and Ding L (1996) Discussion on the uplift process and mechanism of the Qinghai-Tibet Plateau (in Chinese). *Scientia Sinica(Terrae)* 04: 289–295.